

DC-switchable and single-nanocrystal-addressable coherent population transfer

Deniz Günceler and Ceyhan Bulutay¹

Department of Physics, Bilkent University, 06800 Bilkent, Ankara, Turkey.

Achieving coherent population transfer in the solid-state is challenging compared to atomic systems due to closely spaced electronic states and fast decoherence. Here, within an atomistic pseudopotential framework, we theoretically demonstrate the stimulated Raman adiabatic passage for embedded silicon and germanium nanocrystals. The transfer efficiency spectra displays characteristic Fano resonances. By exploiting the Stark effect, we predict that transfer can be switched off with a DC voltage. Furthermore, as the population transfer is highly sensitive to structural variations, with a choice of a sufficiently small two-photon detuning bandwidth, it can be harnessed for addressing individual nanocrystals within an ensemble.

PACS numbers: 78.67.Bf, 78.67.Hc, 42.50.Hz

The control of the dynamics of quantum systems using coherent optical beams lies at the heart of quantum information technologies (for recent reviews, see Refs. 1 and 2). Among several alternatives, the stimulated Raman adiabatic passage (STIRAP) offers a certain degree of robustness in atomic systems with respect to laser parameter fluctuations.³ Moreover, it is not phase sensitive unlike the other coherent control approaches.¹ Its solid-state implementation possesses further advantages such as addressability of the functional units due to lack of free atomic motion, in addition to high density and controlled scalability. Along this direction, researchers have demonstrated STIRAP in $\text{Pr}^{+3}:\text{Y}_2\text{SiO}_5$ crystal,^{4,5} and $\text{Tm}^{+3}:\text{YAG}$ crystal,⁶ all at cryogenic temperatures. Next obvious milestone is to demonstrate STIRAP in nanocrystals (NCs) embedded in a host lattice. Compared to rare-earth doped ions in inorganic solids,^{4–6} NCs bring further flexibility in the design of the functional units by tailoring the physical parameters such as material composition, size, shape, strain and external fields. The challenge with NCs is that the charge degrees of freedom is more susceptible to decoherence compared to the atomic systems.^{7,8}

In this work we consider silicon and germanium NCs embedded in silica. Our aim here is to explore from a theoretical standpoint the intricacies as well as new opportunities for STIRAP in this system. For the level of theory, we avoid the standard electronic structure approach that combines the 2-band (or even 8-band) $k \cdot p$ technique with the envelope function approximation (for a recent example, see Ref. 9), even though it was shown to yield results with qualitative deficiencies in lower dimensions,¹⁰ let alone their poor performance for the highly excited states. As both of these issues are critical for our work, the energy levels, wave functions and dipole matrix elements are computed within a well-tested atomistic pseudopotential framework (for details, see Ref. 11 and references therein). The spin-orbit interaction is particularly included, since this coupling among closely spaced levels can potentially affect the transfer efficiency.

To set the stage, we first discuss the constraints imposed by decoherence on our system. The ultimate deco-

herence mechanism is the radiative recombination. The typical radiative lifetime of Si and Ge NCs is in the microsecond range whereas for direct band gap semiconductors this is in the nanosecond range.¹² Another recombination channel, in case multiple electrons get excited by a strong laser pulse, is the Auger process. According to our recent theoretical estimation for the excited-electron configuration of Auger recombination in Si and Ge NCs, this lifetime is in the range of sub-nanoseconds.¹³ An even more critical decoherence channel in NCs is the acoustic phonon scattering.^{7,8} For the case of InGaAs quantum dots, Borri *et al.* have demonstrated close to radiative limit linewidth at 7 K, corresponding to a dephasing time of 630 ps.¹⁴ In Si NCs, Sychugov *et al.* have shown that the linewidth can also be as sharp as direct band gap materials, reaching 2 meV at 35 K.¹⁵ A similar system is the excited Rydberg states² of phosphorus-doped silicon having an extend of ~ 10 nm for which a dephasing time of ~ 320 ps is very recently predicted.¹⁶ Guided by these reports, we aim for a complete STIRAP in less than 300 ps so that at sufficiently low temperatures of a few Kelvins this can beat the decoherence clock in Si and Ge NCs. Admittedly, this is a cautiously optimistic estimate, nevertheless a worse case can still be accommodated by further scaling the pulse widths and laser powers accordingly; thanks to high-field tolerance of silica embedded NCs.

The crux of STIRAP is based on the simple three-level structure which is faithfully realized by atomic systems.³ In the case of NCs, we have to consider multiple intermediate^{17,18} and final states, whereas we assume a single initial state, the highest occupied molecular orbital (HOMO). However, we assure by selecting the interaction parameters such that the maximum probability of finding a sub-HOMO electron in the conduction band, had the interaction only involved that electron, is below 10^{-9} %. As another technical detail, for small NCs the confinement energy dominates so that the excitonic effects can be ignored.⁸ Furthermore, since ideally the intermediate state is not populated, many-body effects due to Pauli blocking can be neglected (see, Ref. 9 for including these effects).

We base our discussions on a 2.1 nm Si NC and a Ge NC with a 1.5 nm diameter, purposely selected because of their similar band gaps of 2.74 eV and 2.80 eV, respectively. Considering the oscillator strength of the transitions, we adopt different schemes for the two NCs. For 1.5 nm Ge NC the HOMO to lowest unoccupied molecular orbital (LUMO) transition is quite strong, therefore, we utilize the ladder scheme where the electron is transferred from the HOMO state to the LUMO+28 state (0.511 eV above LUMO) via the LUMO state. For 2.1 nm Si NC, we utilize a Λ scheme where the electron is transferred from the HOMO state to the LUMO state via the LUMO+30 state (0.937 eV above LUMO). For the pump and Stokes pulses, we use counterintuitively time-ordered Gaussian profiles³ giving rise to equal peak Rabi frequencies with values 0.35 THz and 0.55 THz for Si and Ge NCs, respectively. Both pulses are linearly polarized but in different special directions to optimize the transfer. We refer to Table I for the other laser parameters.

TABLE I. Laser parameters optimized for STIRAP for the 2.1 nm Si, and 1.5 nm Ge NCs. The incident electric fields are specified for free-space medium. Delay refers to time between the peaks of the Stokes and pump pulses.

	E-field (MV/m)	Wavelength (nm)	FWHM (ps)	Delay (ps)
Si NC				
Pump	155.69	336.9		
Stokes	5.8954	1323	90	75
Ge NC				
Pump	32.325	442.4		
Stokes	92.810	1481	60	50

The transfer efficiency as a function of pump detuning is plotted in Fig. 1. The first observation we make is that the transfer efficiency is superior when the two-photon resonance condition is satisfied. This observation is well documented in literature.³ The central peaks for the two-photon resonance case, for the most part, exhibit a typical Breit-Wigner lineshape. When the system has two-photon detuning, the central peak deforms into a plateau, where the transfer efficiency is essentially constant, and suddenly drops to zero efficiency (cf. upper inset).

Another noteworthy aspect of Fig. 1 is the presence of off-resonance peaks. The detuning values for these peaks correspond to the energy separations between the intermediate states. As the pump and Stokes lasers are detuned from the desired transitions, the system can become resonant with one of the states above or below the targeted intermediate state, hence population transfer can still occur. Because other parameters were optimized for the central peak and not the off-resonance ones, these peaks are usually not as tall or wide. Also since there are no states immediately below LUMO (ladder scheme), for the 1.5 nm Ge NC there are no off-resonance peaks under negative detuning. The peaks other than the central all display the asymmetrical well-known Fano

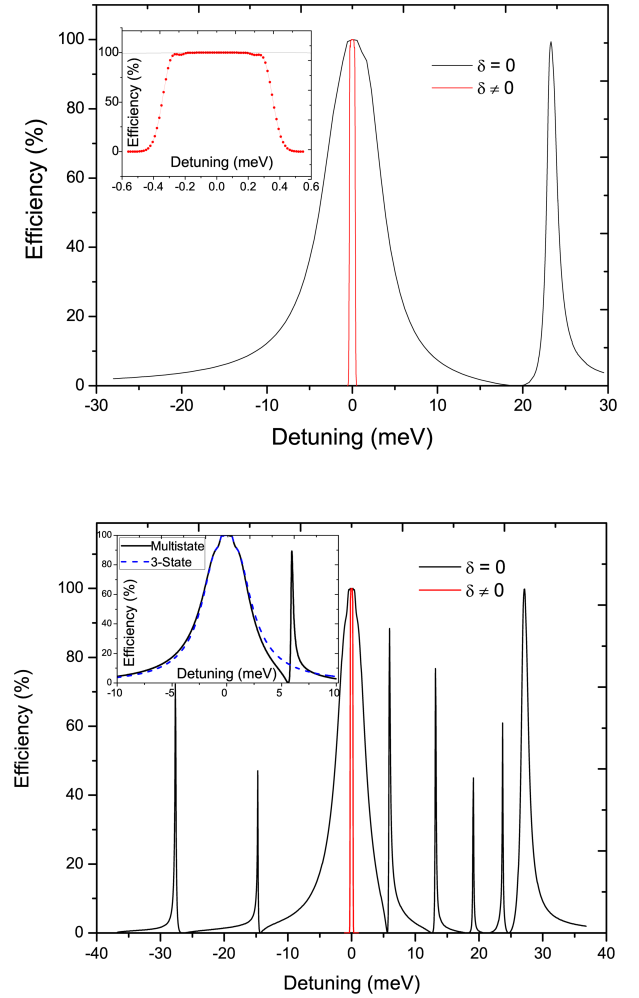


FIG. 1. The population transfer efficiency as the pump laser is detuned from resonant transmission for the 1.5 nm Ge NC (top) and the 2.1 nm Si NC (bottom), with ($\delta = 0$) and without two-photon resonance ($\delta \neq 0$). The inset in the upper graph is a close-up for the central peak; the inset in the lower graph is described in the text.

lineshape.¹⁹ In a similar context, this was observed in the tunnelling induced transparency in quantum well intersubband transitions.²⁰ It arises from two paths interfering with opposite phase on one of the two sides of the resonance. This is illustrated in the lower inset of Fig. 1: When the detuning is not enough to reach any neighbors of the ‘desired’ intermediate state, the calculations made without considering any neighbors agree very well with the full calculation. However, as soon as there is enough detuning to transfer the electron through one of the neighboring states, the neighbors-removed treatment cannot reproduce the dip right before the second peak in the solid line which occurs due to the interference between the chosen intermediate state and its neighbor.

Next, in Fig. 2 we investigate the effect of an external DC electric field.²¹ Here, for the 2.1 nm Si NC we see that for small fields, the transfer efficiency is not af-

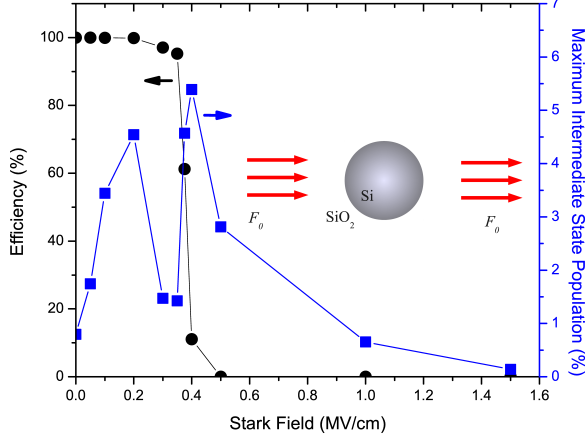


FIG. 2. Effect of DC Stark field on the overall transfer efficiency and maximum intermediate state population for the 2.1 nm Si NC. Lines are only to guide the eyes.

ected, but the intermediate population pile-up increases. After a critical field of 0.35 MV/cm, transfer efficiency rapidly drops to zero. We observed that the system is robust against changes in the dipole matrix elements, hence Rabi frequencies are not significantly altered by the DC field. On the other hand, NC energy levels undergo significant Stark shifts, the valence states being more so compared to conduction states, as revealed by our recent work.²² We checked that in this field range it does not give rise to a level crossing between HOMO and the underlying states. Hence, the primary mechanism responsible for this switching is the Stark shift-induced two-photon detuning, something STIRAP is very sensitive to. For the zero-field case, a detuning of 0.3 meV is enough to destroy STIRAP. This value of Stark shift is reached at 0.5 MV/cm, after which the population transfer is quenched.

Based on the prime importance of two-photon detuning, in Fig. 3 we plot for the 2.1 nm Si NC its variation with respect to time delay between Stokes and pump pulses. As the overlap between these pulses is reduced the two-photon bandwidth first increases up to a delay of 80 ps, beyond which it retracts back, as expected from the fundamental principles of STIRAP that demands a non-zero overlap between the two pulses.³ The upper inset shows the build-up of the intermediate-state population away from the two-photon resonance.

Finally, we focus on the NC's structural sensitivity. Starting with its shape, we consider NCs of the same number of atoms (hence, volume) but with different asphericities as quantified by the ellipticity parameter, e . Denoting a and b as the equatorial radii and c as the polar radius, for oblate spheroids ($a = b > c$) $e = \sqrt{1 - c^2/a^2}$, whereas for prolate spheroids ($a = b < c$) we define it to be *negative* as $e = -\sqrt{1 - a^2/c^2}$. The lower inset of

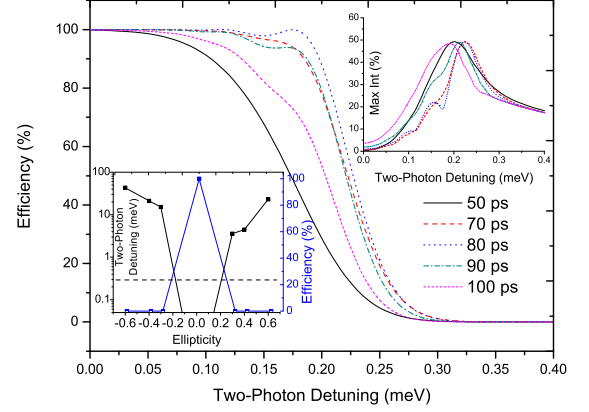


FIG. 3. The variation of two-photon detuning versus transfer efficiency for different time delays between Stokes and pump pulses for the 2.1 nm Si NC. Upper inset displays its effect on the maximum intermediate-state population. Lower inset illustrates the effect NC ellipticity on the two-photon detuning and transfer efficiency (Lines are only to guide the eyes); the horizontal dashed line marks the critical 0.3 meV two-photon detuning level.

Fig. 3 vividly displays the fact that the transfer is lost as the shape of the NC is deformed from the originally targeted geometry to which STIRAP was optimized (here spherical). The variation of only two surface atom positions ($e=0.3$ case) is enough to displace the electronic states away from the tolerable two-photon detuning window. Likewise, we observed that an incremental change in the size of the NC by including the next shell of atoms (not shown) results in a similar loss of transfer. These indicate that practically STIRAP will be locked only to the *single* NC that it is tuned to.

In conclusion, within an atomistic electronic structure framework we show that STIRAP can be achieved in small Si and Ge NCs. Due to dense electronic states it displays a train of Fano resonances. The transfer can be abruptly switched off with a DC voltage by introducing Stark shifts that sufficiently detunes the two-photon resonance. Finally, we demonstrate the sensitivity of the transfer efficiency with respect to structure of the NC which can be instrumental in addressing a single NC among an ensemble having inherent size, shape and even local strain fluctuations.

The partial support from the European FP7 Project UNAM-Regpot Grant No. 203953 is acknowledged.

¹P. Král, I. Thanopoulos, and M. Shapiro, Rev. Mod. Phys. **79**, 53 (2007).

²M. Saffman, T. G. Walker, and K. Mølmer, Rev. Mod. Phys. **84**, 2313 (2010).

³K. Bergmann, H. Theuer, and B. W. Shore, Rev. Mod. Phys. **70**, 1003 (1998).

⁴J. Klein, F. Beil, and T. Halfmann, Phys. Rev. Lett. **99**, 113003 (2007).

- ⁵H.-H. Wang, L. Wang, X.-G. Wei, Y.-J. Li, D.-M. Du, Z.-H. Kang, Y. Jiang, and J.-Y. Gao, Appl. Phys. Lett. **92**, 041107 (2008).
- ⁶A. L. Alexander, R. Lauro, A. Louchet, T. Chanelière, and J. L. Le Gouët, Phys. Rev. B **78**, 144407 (2008).
- ⁷T. Takagahara, Phys. Rev. B, **60**, 2638 (1999).
- ⁸J. Förstner, C. Weber, J. Danckwerts, and A. Knorr, Phys. Rev. Lett. **91**, 127401 (2003).
- ⁹J. Houmark, T. R. Nielsen, J. Mørk, and A.-P. Jauho, Phys. Rev. B, **79**, 115420 (2009).
- ¹⁰D. M. Wood and A. Zunger, Phys. Rev. B **53**, 7949 (1996).
- ¹¹C. Bulutay, Phys. Rev. B **76**, 205321 (2007).
- ¹²C. Delerue and M. Lannoo, *Nanostructures: Theory and Modelling* (Springer-Verlag, Berlin, 2004).
- ¹³C. Sevik and C. Bulutay, Phys. Rev. B **77**, 125414 (2008).
- ¹⁴P. Borri, W. Langbein, S. Schneider, U. Woggon, R. L. Sellin, D. Ouyang, and D. Bimberg, Phys. Rev. Lett. **87**, 157401 (2001).
- ¹⁵I. Sychugov, R. Juhasz, J. Valenta, and J. Linnros, Phys. Rev. Lett. **94**, 087405 (2005).
- ¹⁶P. T. Greenland, S. A. Lynch, A. F. G. van der Meer, B. N. Mordin, C. R. Pidgeon, B. Redlich, N. Q. Vinh, and G. Aeppli, Nature, **465**, 1057 (2010).
- ¹⁷C. E. Carrol and F. T. Hioe, Phys. Rev. Lett. **68**, 3523 (1992).
- ¹⁸N.V. Vitanov and S. Stenholm, Phys. Rev. A **60**, 3820 (1999).
- ¹⁹U. Fano, Phys. Rev. **124**, 1866 (1961).
- ²⁰H. Schmidt, K. L. Campman, A. C. Gossard, and A. Imamoğlu, Appl. Phys. Lett. **70**, 3455 (1997).
- ²¹Through out this work we quote the *matrix* DC electric fields, i.e., outside the NC in the embedding region of silica. For further details we refer to Ref. 22.
- ²²C. Bulutay, M. Kulakci, and R. Turan, Phys. Rev. B **81**, 125333 (2010).